Super cold-crystallization of sodium iodine in selenium based chalco-halide glasses

Claire Fourmentin, Fabrice Celarie, Yann Gueguen, Louisiane Verger, Xianghua Zhang, Mathieu Rozé, Yann Guimond, Laurent Calvez

Super Cold-Crystallization of Sodium Iodine in Selenium Based Chalco-halide Glasses

Claire Fourmentin[1], Fabrice Celarie[2], Yann Gueguen[2], Louisiane Verger[1], Xiang-Hua Zhang[1], Mathieu Rozé[3], Yann Guimond[3], Laurent Calvez[1]*

[1]Univ Rennes, CNRS, ISCR (Institut des Sciences Chimiques de Rennes) - UMR 6226, F-35000 Rennes, France
[2]Univ Rennes, CNRS, IPR - UMR 6251, F-35000 Rennes, France
[3]Umicore I.R Glass, Z.A du Boulais, 35690, Acigné
*Corresponding author: laurent.calvez@univ-rennes1.fr

Keywords: Chalcohalide glass, Crystallization, Mechanical properties, Isothermal treatment

I. ABSTRACT

Mechanical properties of a chalco-halide glass of the composition $(0.72\ GeSe_2 – 0.28\ Ga_2Se_3)_{75}\ NaI_{25}$ are studied during isothermal treatment below T_g (T_g-60 °C). The evolution of the Young's Modulus (E), the damping (Q^{-1}) and the apparent viscosity (J^{-1}, reverse of the creep rate) during heat treatment show that a structural rearrangement occurs in the glass below T_g. X-Ray diffraction and transmission measurements of the sample after heat treatment highlight the beginning of a super cold crystallization of cubic NaI within the glass after 1 month at T_g-60 °C. After 3 months of heat treatment, NaI crystals of about 31 nm size have been observed in the glass matrix by transmission electron microscopy.

II. Introduction

Se-based chalco-halide glasses can offer a good transparency window from the visible (about 0.6 µm) to the infrared (up to 16 µm), making them good candidates for use in infrared optics[1 2 3]. However, their application is often limited because of their fast aging due to oxidation and physical relaxation[4].
Halide atoms introduced into the $GeSe_2$-Ga_2Se_3 chalcogenide glass network induce a decrease into the network connectivity because of their non-bridging nature. Thus, some mobility is offered to the cations inside the network, and for this reason, the $GeSe_2$-Ga_2Se_3-MX glass system was investigated as a candidate for strengthening physical characteristics of the glass by ionic exchange[5,6].
Recently, the $(0.72\ GeSe_2 – 0.28\ Ga_2Se_3)_{75}\ NaI_{25}$ chalco-halide glass was studied to obtain gradient refractive index lenses by ionic exchange[7]. This glass composition showed a crystallization during the ionic exchange at a temperature below glass transition (T_g). This phenomena was already observed in metallic glasses[8,9]. It is explained by a sufficient mobility of elements at low temperature ($<T_g$) inside the glass, due to the metallic nature of the bonds, compared to silicate glasses, where the bonds are covalent. It was also studied in $Ca(PO_3)_2$[10] bulk glass, or created by thermal poling in a silicate glass K_2O-TiO_2-SiO_2[11].
Crystallization below T_g has not been observed yet in chalcogenide glasses, but a recent study, by Klym et al.[12], highlighted a « cold crystallization », which is a crystallization near T_g, but still above, in the $80\ GeSe_2 – 20\ Ga_2Se_3$ glass. Glasses were heat treated at T_g + 10 °C from 0 to 100 h, and showed a crystallization of $GeGa_4Se_8$ and Ga_2Se_3 nanoparticles starting from 25 h of thermal treatment.
In this work, we studied the cold crystallization below T_g of the $(0.72\ GeSe_2 – 0.28\ Ga_2Se_3)_{75}\ NaI_{25}$ glass during and after isotherm treatments at T_g-60 °C.

III. Methods

The $(0.72\ GeSe_2 – 0.28\ Ga_2Se_3)_{75}\ NaI_{25}$ glass was prepared by following the ordinary melt-quenching route. The pure raw elements (Ge, Ga, Se: 5N and NaI: 2N) were weighted following the stoichiometric proportions and placed in a silica tube of 10 mm inner diameter. The ampoule was sealed under secondary vacuum (10^{-5} bar) and placed in a

rocking furnace where the raw materials were heated up to 870 °C for 10 h. The molten mixture was then quenched in water before being annealed for 3 h at T_g-10 °C to relax mechanical constrains in the formed glass.
Rod shaped samples of 1 cm long and 1 cm diameter were heat treated in a ventilated furnace for 3 months at T_g-60 °C. Slices of 5 mm thick were cut and polished for characterizations.
Characteristic temperatures of the glass (glass transition temperature: T_g, crystallization onset temperature: T_x) were measured on bulk samples by Differential Scanning Calorimetry (DSC 2010 TA Q20), with a heating rate of 10 °C/min.
X-ray diffraction (XRD) were conducted on bulk samples using a PANalytical X'Pert Pro in Bragg-Brentano geometry with an excitation wavelength Cu $K_{\alpha1, \alpha2}$. Samples were preliminary polished after heat treatment in order to avoid a potential surface oxidation. The angular range used is from 5 ° to 120 ° 2θ with a step size of 0.026 ° and an acquisition time of 400 seconds of effective counting time. Le Bail profile refinement using the FullProf suite program was carried out[13].
Transmission ranges were measured on 5 mm thick polished samples using UV–Vis (Perkin Elmer) and a FTIR (Bruker Vector 22) spectrophotometers.
Images were taken by a Jeol JEM 2100 HR transmission electron microscope (TEM) with a LaB_6 electron source and an accelerating voltage of 200 kV. In order to perform the analysis, the glass heat treated for 3 months at T_g-60 °C was crushed just before analysis in anhydrous ethanol and then deposited on a copper grid covered with a carbon film.
Glass density has been measured using the classical Archimedes technique.
Hardness (Hv) was measured using a Vickers indenter (Matsuzawa) using a constant force of 100 g for a duration of 5 s. The reported value is an average of ten measurements.

The Young's Modulus (E) and the Damping (Q^{-1}) measurement during heat treatment were performed in a rod-shaped glass sample of 6.26 cm long and 1 cm of diameter. Measurements were recorded during 37 days (1 month) at T_g-60 °C. Values for E was calculated using flexural frequencies by resonance spectroscopy (RFDA, IMCE, Belgium) in a furnace (Nabertherm, Lilienthal, Lower Saxony, Germany) controlled by a software (RFDA HT1050). For a rod-shaped specimen, E is calculated as followed[14]:

$$E = 0.9465 * \rho * f_f^2 \left(\frac{L^4}{e^2}\right) T \quad (1)$$

With E the Young's Modulus (Pa), ρ the density of the specimen (kg.m^{-3}), f_f the fundamental flexural resonant frequency of the rod (Hz), L the length of the rod (mm), e the diameter rod (mm) and T a correction factor, very close to 1. The Q^{-1} factor is determined for each vibration mode i (f_f corresponds to the first mode), according to the recorded acoustic signal x:

$$x(t) = \sum_i A_i e^{-k_i t} \sin(2\pi f_i t + \emptyset_i) \quad (2)$$

with A_i the signal amplitude for the mode i, k_i the corresponding exponential damping of the oscillation, and $\emptyset_i$ the initial phase. For each k the corresponding Q^{-1} is calculated as[15] :

$$Q^{-1}{}_i = \frac{k_i}{\pi f_i} \quad (3)$$

Creep indentation measurements were realized on rod shaped samples of 8 mm long and 10 mm diameter for 55 h at Tg-60 °C by home-made instrumented indentation[16]. This measurement allows to access to the creep compliance $C(t)$, which would be (the stress is not constant during an indentation creep test[16]) the ratio between an applied constant stress σ during a conventional creep test and the resulting strain ε: $C(t) = \varepsilon(t)/\sigma$. In the stationary regime, the slope of $C(t)$ (*i.e.:* the creep rate) is the reciprocal ($1/\eta$) of the viscosity (η). We can define $J^{-1}(t) = 1/\dot{C}(t)$, thus:

$$J^{-1}(t) = \frac{\sigma}{\dot{\varepsilon}(t)} \quad (4)$$

Above the glass transition, a glass will always have a J^{-1} that increases over time: this is the primary creep regime. J^{-1} eventually stabilizes at a value that corresponds to the viscosity ($\eta = \lim_{t\to\infty} J^{-1}(t)$). J^{-1} is thus, in a sense, the apparent viscosity of the glass.

Under the glass transition, due to structural relaxation, the viscosity increases with time, which induces a longer time to stabilization, but a J^{-1} whose rate (dJ^{-1}/dt) continuously decreases.

IV. Results and discussion

1. Thermal properties and density of the base glass

Thermal characteristics and density of the base glass containing 25 mol. % of NaI are presented in **Table 1.** Thermal properties of the glass show that this composition is supposed to be stable face to crystallization (ΔT >100 °C)

Table 1 : Thermal properties and density of the $(0.72\ GeSe_2\text{-}0.28\ Ga_2Se_3)_{75} – (NaI)_{25}$ glass

	$(0.72\ GeSe_2\text{-}0.28\ Ga_2Se_3)_{75} – (NaI)_{25}$
T_g (± 2 °C)	310
T_x (± 2 °C)	462
T_p (± 2 °C)	483
T_x-T_g (°C)	152
Density (±0,02 g.cm^{-3})	4,21
Hv (±8 kg.mm^{-2})	143

2. Mechanical study during an isothermal treatment at T_g-60 °C

Figures 1 a and 1 b show the evolution of the Young's modulus (E) and the damping (Q^{-1}) of a glass of composition $(0.72\ GeSe_2\ -\ 0.28\ Ga_2Se_3)_{75}\ (NaI)_{25}$ during an isothermal treatment at 250 °C for 37 days.

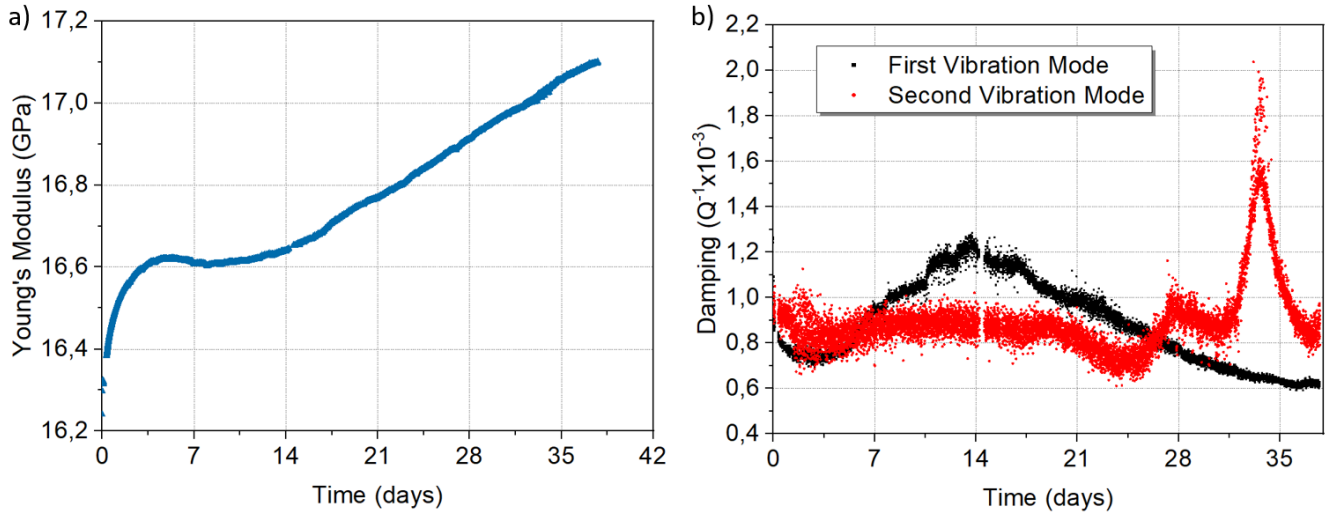

Figure 1 : a) Evolution of the Young's modulus and b) damping factor of the first and second vibration mode of the glass $(0.72\ GeSe_2\ -\ 0.28\ Ga_2Se_3)_{75}\ NaI_{25}$ during an isothermal heat treatment at T_g-60 °C for 37 days.

Increases in Young's modulus are observed, the first from 0 to 3.5 days and the second from 7 days, with apparent

changes in slope after 14 and 33 days. Comparing the glass before and after the isothermal treatment, there is a 5 % increase in Young's modulus (0.85 GPa).
During the isotherm, the observation of the evolution of the damping of the natural frequencies of vibrations as a function of time (**Figure 1 b**) shows peaks with maxima. Those maxima seem to corroborate with the changes in slopes observed during the evolution of Young's modulus as a function of time (14 days and 33 days).
The increase in Young's modulus, as well as the damping peaks, can be indicative of different mechanisms such as atomic mobility, phase separation, or the onset of crystallization[17,18].

The evolution of the apparent viscosity J^{-1} as a function of time during an isotherm was measured for glass (0.72 $GeSe_2$ - 0.28 $Ga_2Se_3)_{75}$ $(NaI)_{25}$. The measurement was run at T_g-60 °C for 55 h, this temperature being reach from room temperature at 10 K/min. Results are presented in **Figure 2**. They are compared to the creep curves of a window glass (Planilux®, Saint Gobain) simulated around its T_g based on structural relaxation and viscoelastic data from the literature[19]. The simulation is made with glasses cooled down from 1000 K to room temperature at 10 K/min and heated up at 10 K/min to the creep temperatures.

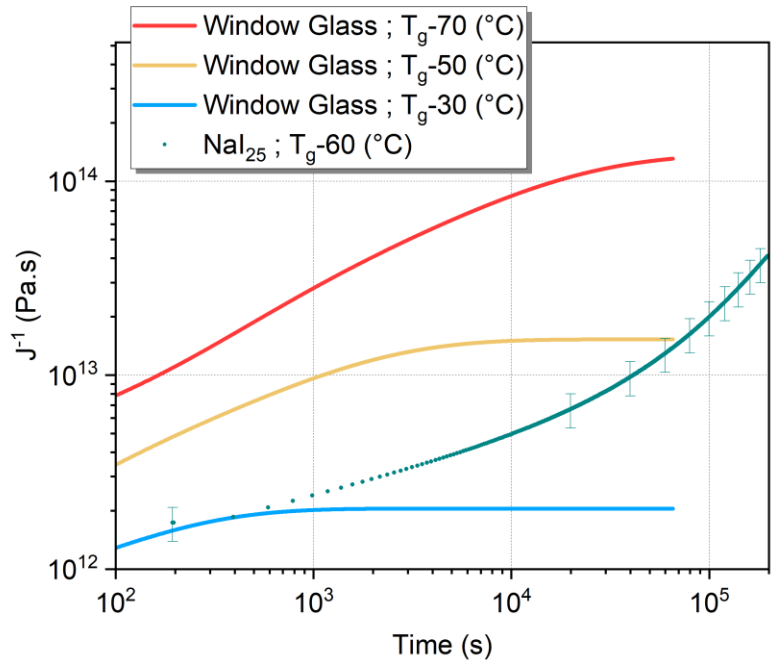

Figure 2 : Comparison of the evolution of the apparent viscosity (J^{-1}) as a function of time of a window glass (Planilux, Saint Gobain) below T_g (T_g-30 °C, T_g-50 °C and T_g-70 °C) and glass (0.72 $GeSe_2$ - 0.28 $Ga_2Se_3)_{75}$ $(NaI)_{25}$ at T_g-60 °C.

Below T_g, the window glass exhibits the combined effects of the primary regime and the relaxation, which induce a continuous increase of J^{-1} ($dJ^{-1}/dt>0$), but increasingly slow ($d^2J^{-1}/dt^2<0$). Eventually, the window glass at T_g-30 °C and T_g-50 °C reaches the plateau ($dJ^{-1}/dt=0$) corresponding to their equilibrium viscosity. This plateau is reached after a much longer time for the window glass at T_g-70 °C. For the (0.72 $GeSe_2$ - 0.28 $Ga_2Se_3)_{75}$ $(NaI)_{25}$ glass, J^{-1} increases continuously, but we can see that its growth accelerates ($d^2J^{-1}/dt^2>0$). This acceleration can neither be attributed to the primary regime, nor to structural relaxation, both of which will induce a deceleration, as seen for a window glass. On the other hand, this type of acceleration can be observed either during crystallization or during phase separation[20]. Therefore, this acceleration of the increase in viscosity can be due either to the presence of the dispersed crystals in the matrix, and/or to the change in composition of the remaining glassy phase, in case of crystallization, or major phase, in case of phase separation[21].

3. Characterization after an isothermal treatment at T_g-60°C

XRD data and transmission spectrum of (0,72 $GeSe_2$ – 0,28 $Ga_2Se_3)_{75}$ NaI_{25} samples before and after heat treatment at T_g-60 °C for 1 and 3 months are presented in **Figure 3 a, b and c**.

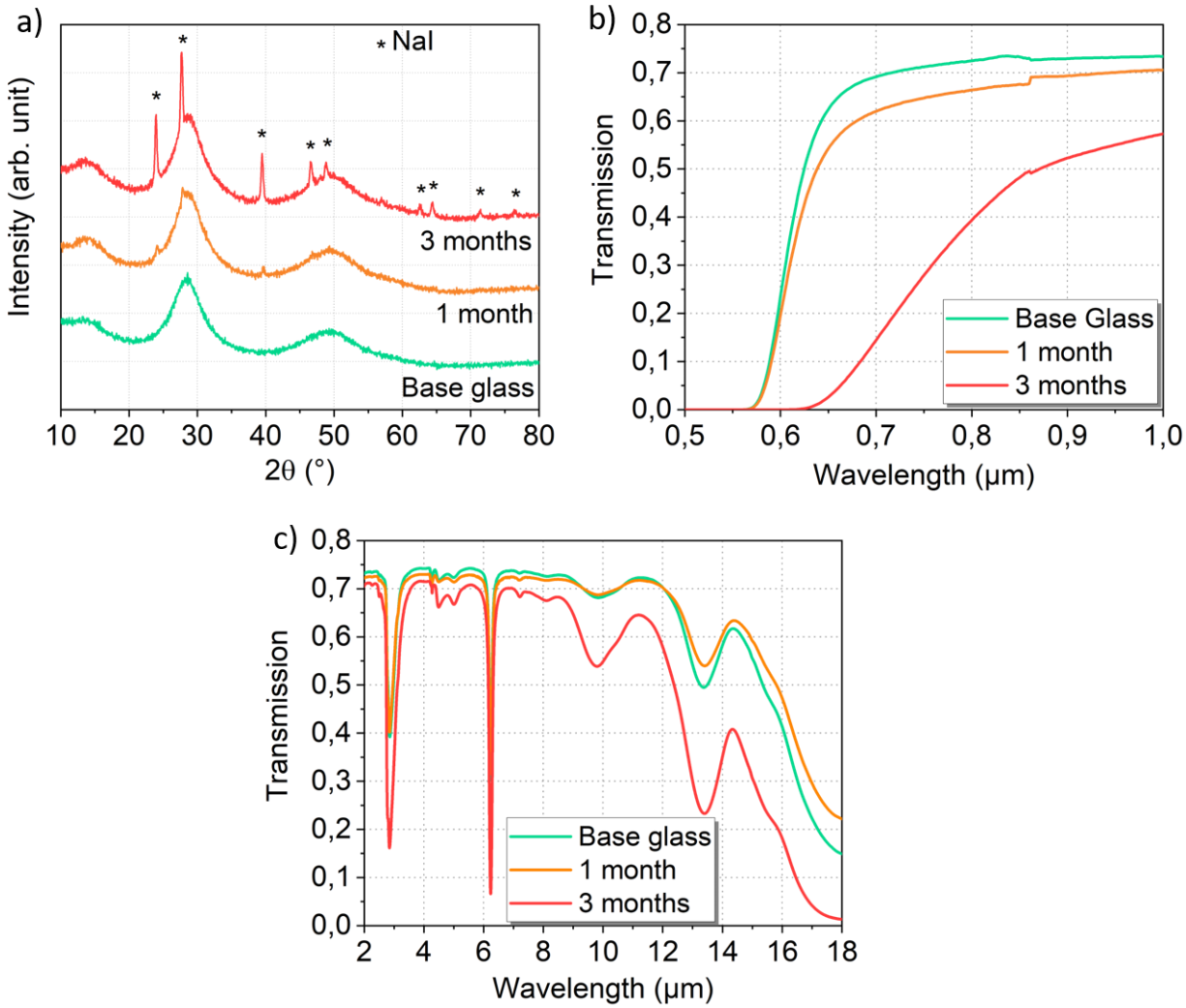

Figure 3 : a) X-ray diffraction patterns, b) Visible-Probe IR transmission and c) IR transmission of $(0.72\ GeSe_2 - 0.28\ Ga_2Se_3)_{75}\ NaI_{25}$ glass before (green) and after 1 month (orange) and 3 months (red) of heat treatment at T_g-60 °C

The base line observed in the XRD pattern (**Figure 3 a**) of the glass is characteristic of an amorphous material. After 1 month of heat treatment, the characteristic peaks of cubic NaI (space group *F m* -3 *m*) start to appear at 24, 27 and 40 ° 2θ. After 3 months, the intensity of the peaks is higher and characteristic NaI peaks are detected beyond 40 ° 2θ. The optical transmission of samples annealed for 1 and 3 months decreases at short wavelength (**Figure 3 b**), attesting the presence of light-scattering submicron particles in the sample. The scattering is more important for the sample treated for 3 months at 250 °C than for the one treated for 1 month. This is consistent with the XRD patterns showing a higher amount of crystals after 3 months. Infrared transmission (**Figure 3 c**) in the atmospheric band II (3-5 µm) and III (8-14 µm) are practically unchanged for the glass after 1 month of heat treatment. For the sample annealed for 3 months, an overall decrease of the IR transmission is observed, with an increase in the absorption of oxide bands at 2.9, 6.3, 9.8 and 13 µm.

In order to determine the average crystal size, profile refinement using the Le Bail method without structural constraints was performed on the XRD pattern of the sample treated for 3 months (**Figure 4 a**). Using the instrumental resolution function, the Scherrer formula gives a global average apparent size of diffracting crystallites around 38 nm.

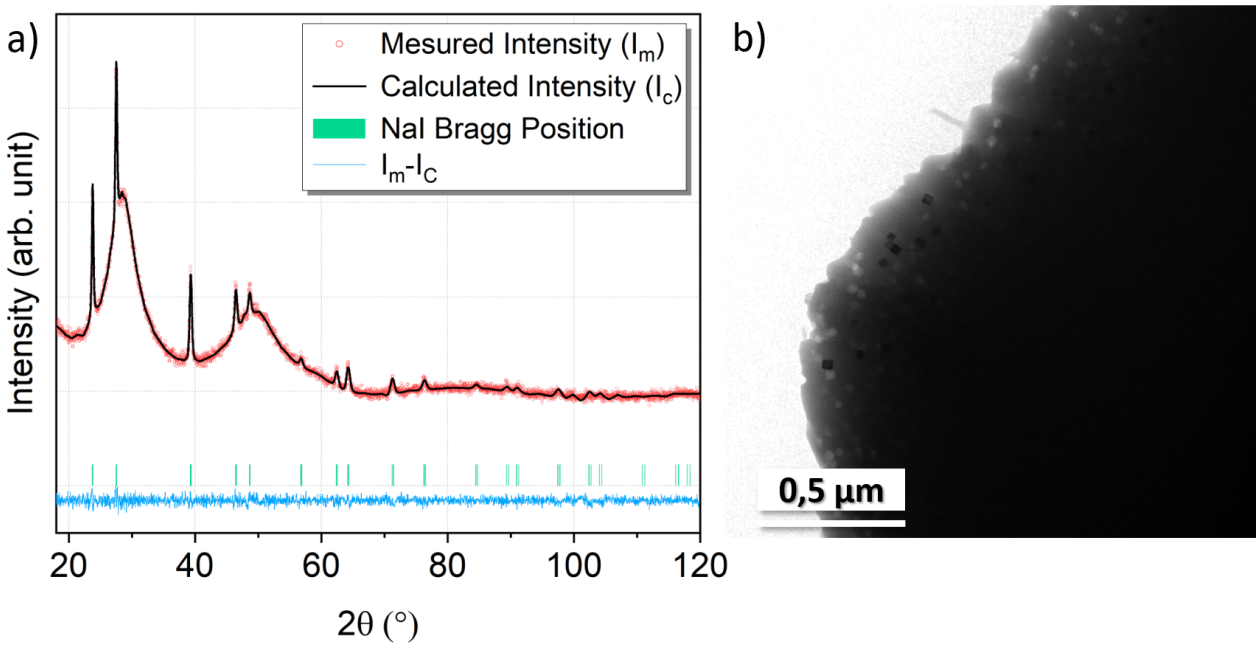

Figure 4 : a) Le Bail refinement of the X-ray diffraction pattern and b) TEM imaging of (0.72 $GeSe_2$ - 0.28 Ga_2Se_3)$_{75}$ $(NaI)_{25}$ glass heat treated at T_g-60 °C for 3 months

Small black cubes are observed in TEM images of the sample annealed for 3 months. Selected area electron diffraction patterns were performed showing the main inter-reticular distances of NaI, without any correspondence with other compounds such as ß-Ga_2Se_3, GeSe, $GeSe_2$. Therefore, the black cubes correspond to NaI crystals, embedded in a glassy matrix. The white cubes are inclusions left by NaI crystals that have degraded under the electron beam. An average size of 31 nm is measured on the TEM images for the NaI crystals, consistent with the value obtained by XRD.

V. Conclusion

Mechanical characterizations combining RFDA measurements and instrumented indentation during an isotherm at T_g-60 °C have shown that a structural rearrangement process associated with an increase of the Young's Modulus takes place at this temperature in the (0.72 $GeSe_2$ - 0.28 Ga_2Se_3)$_{75}$ NaI_{25} glass composition, either in the form of crystallization or phase separation. However, it is not possible to conclude from these data whether only one of these mechanisms takes place, or whether both occur.

The characterizations of the glass after undergoing the isotherm at T_g-60 °C for 1 month and 3 months, reveal a super cold crystallization of cubic NaI crystals below T_g in the samples.

The chalco-halide glass of composition (0.72 $GeSe_2$ - 0.28 Ga_2Se_3)$_{75}$ NaI_{25} thus presents a crystallization phenomenon under the glass transition temperature after heat treatment times higher than 1 month. This composition is probably at the limit of supersaturation of NaI incorporation in the glass matrix, which therefore tends crystallize. However, this glass maintains good IR optical properties due to the low scattering induced by the small size of the crystals.

VI. Funding

The authors are grateful to the French DGA, Direction Générale de l'Armement (project ANR-18-ASTR-0014) for supporting this work. Authors would like to acknowledge the IUF (Institut Universitaire de France). This publication is supported by the European Union through the European Regional Development Fund (ERDF), the Ministry of Higher Education and Research, the french region of Brittany and Rennes Métropole.

VII. Acknowledgements

Ludivine Rault is acknowledged for Transmission Electron Microscopy experiments performed on THEMIS platform (ScanMAT, UAR 2025 University of Rennes 1-CNRS, CPER-FEDER 2007–2014).

VIII.Reference

1. Heo, J. Chalcohalide glasses for infrared fiber optics. *Opt. Eng.* **30**, 470 (1991).
2. Calvez, L., Ma, H. L., Lucas, J. & Zhang, X. H. Glass and glass-ceramics transparent from the visible range to the mid-infrared for night vision. *IJNT* **5**, 693 (2008).
3. Calvez, L. *et al.* Influence of gallium and alkali halide addition on the optical and thermo–mechanical properties of $GeSe_2$-Ga_2Se_3 glass. *Appl. Phys. A* **89**, 183–188 (2007).
4. Jensen, M., Smedskjaer, M. M., Wang, W., Chen, G. & Yue, Y. Aging in chalcohalide glasses: Origin and consequences. *Journal of Non-Crystalline Solids* **358**, 129–132 (2012).
5. Calvez, L. *et al.* Strengthening of chalco-halide glasses by ion exchange. *Journal of Non-oxide and Photonic Glasses* **1**, 30–37 (2009).
6. Calvez, L. *et al.* Controlled crystallization in Ge-(Sb/Ga)-(S/Se)-MX glasses for infrared applications. *Journal of the Ceramic Society of Japan* **116**, 1079–1082 (2008).
7. Fourmentin, C. *et al.* IR GRIN lenses prepared by ionic exchange in chalcohalide glasses. *Sci Rep* **11**, 11081 (2021).
8. Köster, U. & Meinhardt, J. Crystallization of highly undercooled metallic melts and metallic glasses around the glass transition temperature. *Materials Science and Engineering: A* **178**, 271–278 (1994).
9. Louzguine, D. V. & Inoue, A. Crystallization behaviour of Al-based metallic glasses below and above the glass-transition temperature. *Journal of Non-Crystalline Solids* **311**, 281–293 (2002).
10. Abe, Y., Arahori, T. & Naruse, A. Crystallization of $Ca(PO_3)_2$ Glass Below the Glass Transition Temperature. *Journal of the American Ceramic Society* **59**, 487–490 (1976).
11. Lipovskii, A. A., Melehin, V. G., Redkov, A. V., Reshetov, I. V. & Tagantsev, D. K. Crystallization of K2O-TiO_2-SiO_2 glass below glass transition by poling. *Journal of Non-Crystalline Solids* **571**, 121081 (2021).
12. Klym, H. *et al.* 'Cold' crystallization in nanostructurized 80GeSe2-20Ga2Se3 glass. *Nanoscale Res Lett* **10**, 49 (2015).
13. Rodríguez-Carvajal, J. Recent advances in magnetic structure determination by neutron powder diffraction.

Physica B: Condensed Matter **192**, 55–69 (1993).

14. Kita, H., Kitano, I., Uchida, T. & Furukawa, M. Light-Focusing Glass Fibers and Rods. *Journal of the American Ceramic Society* **54**, 321–326 (1971).
15. Nowick, A. S. *Anelastic Relaxation In Crystalline Solids*. (Elsevier, 2012).
16. Bernard, C., Keryvin, V., Sangleboeuf, J.-C. & Rouxel, T. Indentation creep of window glass around glass transition. *Mechanics of Materials* **42**, 196–206 (2010).
17. Idriss, M., Célarié, F., Yokoyama, Y., Tessier, F. & Rouxel, T. Evolution of the elastic modulus of Zr–Cu–Al BMGs during annealing treatment and crystallization: Role of Zr/Cu ratio. *Journal of Non-Crystalline Solids* **421**, 35–40 (2015).
18. Sant'Ana Gallo, L. *et al.* In situ crystallization and elastic properties of transparent $MgO–Al_2O_3–SiO_2$ glass-ceramic. *Journal of the American Ceramic Society* **100**, 2166–2175 (2017).
19. Carre, H. & Daudeville, L. Numerical Simulation of Soda-Lime Silicate Glass Tempering. *J. Phys. IV France* **06**, C1-185 (1996).
20. Exnar, P. Study of rock glass viscosity in the course of crystallization by a penetration viscometer. in A542–A550.
21. Jabed, A., Meduri, C. S. & Kumar, G. Effect of time on the isothermal viscosity of metallic glass supercooled liquids. *Journal of Alloys and Compounds* **863**, 158067 (2021).